Journal of Applied Polymer Science

Bifunctional cellulose derivatives for the removal of heavy-metal ions and phenols: Synthesis and adsorption studies

Ronglan Wu,[1] Lingyuan Tian,[1] Wei Wang,[1,2] Xiaolin Man[1]

[1]Key Laboratory of Oil and Gas Fine Chemicals, Ministry of Education and Xinjiang Uyghur Autonomous Region, College of Chemistry and Chemical Engineering, Xinjiang University, Urumqi, Xinjiang 830046, China

[2]Centre for Pharmacy and Department of Chemistry, University of Bergen, Bergen N-5007, Norway

Correspondence to: W. Wang (E-mail: wei.wang@kj.uib.no)

ABSTRACT: In this article, we report a study of the design and synthesis of a bifunctional cellulose derivative on the removal of phenols and heavy-metal ions in wastewater treatment. A radical polymerization was performed in an ionic liquid, 1-allyl-3-methylimidazolium chloride, to graft two monomers, butyl methacrylate and 4-vinyl pyridine, on the backbone of cellulose. The effects of the five reaction conditions on the yield of final products were evaluated. The grafted celluloses were characterized by means of Fourier transform infrared spectroscopy, scanning electron microscopy, and thermogravimetric analysis. Adsorption experiments were carried out on the cellulose-*g*-poly(butyl methacrylate-*co*-4-vinyl pyridine) to evaluate the capacity of the removal of 2,4-dichlorophenol (2,4-DCP) and Cu(II) in water. The adsorption isotherms were measured at five temperatures and interpreted by a Langmuir model of adsorption. The thermodynamics of the adsorption suggested that the binding process was mildly exothermic for Cu(II) and endothermic for 2,4-DCP. Kinetic studies were interpreted with a pseudo-second-order adsorption model. The process of the adsorption of 2,4-DCP could be described overall by the model, whereas the adsorption of Cu(II) involved two processes. This was due to adsorption both on the surface and inside the adsorbent. © 2015 Wiley Periodicals, Inc. J. Appl. Polym. Sci. **2015**, *132*, 41830.

KEYWORDS: adsorption; applications; biomaterials; cellulose and other wood products; radical polymerization

Received 17 September 2014; accepted 4 December 2014
DOI: 10.1002/app.41830

INTRODUCTION

We are facing a growing demand for quality water with regard to increasing concerns about public health and environmental quality in many developing counties.[1,2] Because of rapid urbanization and industrialization, a large amount of disposal sewage is produced daily; it requires purification before it is discharged into environment. This calls for the development and implementation of effective methods for wastewater treatment. Currently, broadly applied technologies in wastewater treatment include flocculation, precipitation, adsorption, ion exchange, and reverse osmosis.[3] The removal of pollutants by traditional precipitation processes is often insufficient for meeting pollution control limits, and the use of reverse osmosis technology is quite expensive.[4] Adsorption has become the most feasible method in wastewater treatment, and it is currently being used extensively.[5,6] Adsorbent materials derived from byproducts in agriculture and sea products, such as celluloses, can be used for the effective removal of pollutants in sewage.[7,8] Unmodified cellulose, however, has a very low adsorption capacity for both heavy-metal ions and organic chemicals, and the physical properties of unmodified cellulose are unstable when the cellulose is exposed to harsh chemical or biological environments.[3] Thus, studies of the adsorption of cellulose derivatives have been focused on achieving adequate structural durability and high adsorption capacity.[9,10] These can be achieved by the modification of cellulose.[11]

With regard to grafted celluloses used in the water treatment, most studies have been focused on the adsorption of either heavy metals or organic pollutants.[12,13] As heavy-metal ions and organic chemicals are often present in sewage together, the necessity for developing a material that adsorbs both types of pollutes is in demand for many applications. In this study, we focused on bifunctional cellulose derivatives that were able to absorb both heavy-metal ions and organic wastes. On the basis of the mechanism of adsorption, we introduced 4-vinyl pyridine (4VP) as a metal-binding group and butyl methacrylate (BMA) to interact with organic wastes. The results show that the p(4VP-*co*-BMA) grafted cellulose showed a high adsorption capacity, and the two types of monomers exhibited a synergetic effect on the sorption of Cu(II) and 2,4-dichlorophenol (2,4-DCP).

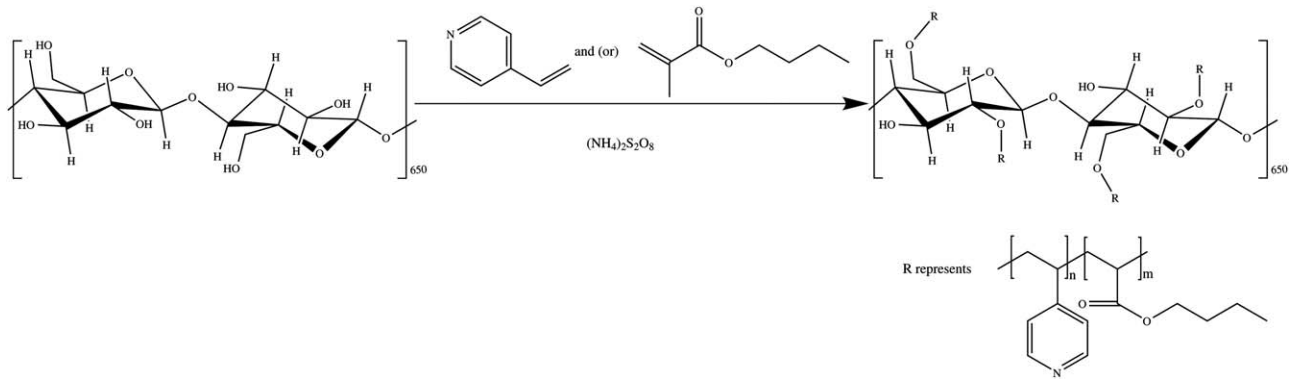

Scheme 1. Synthesis route of the grafted celluloses.

EXPERIMENTAL

Materials

Natural cellulose (bamboo pulp) was purchased from Beiyan Yasong Paper Co. (Chengdu, China). The degree of polymerization of the cellulose was 650, as measured with an Ubbelohde viscometer in a cupriethylenediamine hydroxide solution. *N,N′*-Methylene bisacrylamide (MBA; >98%), ammonium persulfate (APS; >98%), *N,N*-dimethylformamide (>99%), ethanol (>99.5%), and copper(II) sulfate were purchased from Tianjing Chemical Corp. (Tianjing, China). BMA (>98%), 4VP (>99%), and 2,4-DCP (>98%) were purchased from Aladdin Industrial Corp. (Shanghai, China). Poly(vinylidene fluoride) (PVDF) filters with a 0.45-μm pore size were purchased from Yaxin Corp. (Shanghai, China). Stock solutions of HCl and NaOH with concentrations of 0.1 mol/L were prepared and used to adjust the pH in the experiments. The chemicals were used without further purification. Milli-Q water with a resistivity of 18 MΩ cm was used in all of the experiments.

Synthesis

Synthesis of Cellulose-*g*-BMA, Cellulose-*g*-4VP, and Cellulose-*g*-Poly(4VP-*co*-BMA). The cellulose (0.02 g) was dissolved in an ionic liquid (10 g), 1-allyl-3-methylimidazolium chloride, at 80°C. The synthesis of 1-allyl-3-methylimidazolium chloride was followed a procedure reported earlier.[14] Then, 5 mL of dimethylformamide was added to the solution. After stirring, the color of the solution appeared to be slightly amber.

BMA (0.875 g) was added to the cellulose solution, which was then mixed with MBA and APS at a weight ratio of 5:0.5. The reaction temperature was controlled at a certain temperature for less than 8 h. The amount of the initiator, the reaction temperature, and the reaction time are discussed further in the Results section (Scheme 1). Thereafter, the temperature of the solution was reduced to room temperature. A large amount of Milli-Q water was charged into the reaction flask. Because the cellulose derivative was insoluble in water, the product precipitated from the solution. The BMA-grafted cellulose was immersed in water for 48 h and then washed thoroughly to remove unreacted monomers. Then, the precipitate were collected and dried *in vacuo* at 60°C.

The same procedure was used to synthesize cellulose-*g*-4VP and cellulose-*g*-poly(BMA-*co*-4VP). The amount of 4VP used to synthesize cellulose-*g*-4VP was 0.980 g. The amount of 4VP used to synthesize the cellulose-*g*-poly(BMA-*co*-4VP) is specified in the first subsection of the Results section. The optimum synthesis conditions were evaluated by grafting percentage (GP) and grafting efficiency (GE), which were determined as follows:

$$\mathrm{GP} = \frac{W_2 - W_0}{W_0} \quad (1)$$

$$\mathrm{GE} = \frac{W_2 - W_0}{W_1} \quad (2)$$

where W_0, W_1, and W_2 represent the weights of the initial cellulose, monomers, and grafted celluloses, respectively.

Characterization

Fourier Transform Infrared (FTIR) Spectroscopy. FTIR spectroscopy of the cellulose, cellulose-*g*-BMA, cellulose-*g*-4VP, and cellulose-*g*-poly(BMA-*co*-4VP) were carried out on an IR Prestige-21 (Shimadzu, Japan). The dried cellulose and grafted cellulose samples were mixed with KBr and compressed to into KBr pellets. The measurements were performed in the wavelength range from 400 to 4000 cm^{-1}.

Scanning Electron Microscopy (SEM). The micrographs of the cellulose and cellulose-*g*-poly(BMA-*co*-4VP) were captured with a scanning electron microscope (Leo 1430 VP, Germany).

Thermogravimetric Analysis (TGA). TGA was carried out on a Q600SDT TGA instrument (TA Instruments, Inc.). The speed of the nitrogen stream was 100 mL/min. The temperature scanning was done in the range of 30–500°C with an increasing rate of 5°C/min.

Adsorption Experiments

Adsorption Isotherm. A series of Cu(II) solutions and 2,4-DCP solutions with various concentrations was prepared by the dissolution of copper sulfate and 2,4-DCP in water, respectively. A 25.00 mL aliquot of Cu(II) or 2,4-DCP solution was mixed with 0.020 g of absorbent in a vial. The vials were then sealed and shaken for 2 h. The adsorption experiments were performed at five temperatures between 293 and 333 K. The concentration of Cu(II) for each sample was then measured with atomic absorption spectroscopy (Shimadzu FTAS-990, Japan). The concentration of 2,4-DCP was measured with ultraviolet–visible spectroscopy (Shimadzu UV-2450, Japan). The amount of solute

adsorbed at equilibrium per gram of adsorbent (q_e) was calculated as follows:

$$q_e = \frac{c_0 - c_e}{W} V \quad (3)$$

where c_0 and c_e are the concentrations of the solute before and after adsorption (mg/L), respectively; V is the volume of the solution (L); and W is the weight of the absorbent (g).

Kinetics of the Adsorption. An amount of 300.0 mg of adsorbent was mixed with 500.0 mL of Cu(II) solution or 2,4-DCP solution with various initial concentrations. The vials were sealed and shaken at 297 K. At each time point, 1.00 mL of supernatant was removed and filtered through a 0.45-μm PVDF membrane before the atomic absorption spectroscopy measurement. The same procedure was followed for the set of 2,4-DCP, and the concentration of 2,4-DCP was determined with ultraviolet–visible spectroscopy. All of the experiments and measurements were conducted twice to ensure accuracy and reproducibility.

RESULTS

The results section is organized as follows: (1) we discuss the synthesis conditions of the three grafted celluloses with regard to the yield of the final products, which include the monomer ratio, reaction temperature, reaction time, amount of initiator, and amount of crosslinker; (2) we present the characterization of the grafted celluloses with FTIR spectroscopy, SEM, and TGA; and (3) we present the results of the adsorption experiments, which include the adsorption isotherms and adsorption kinetics for cellulose-*g*-poly(BMA-*co*-4VP).

Optimum Synthesis Conditions of Cellulose-*g*-Poly(BMA-*co*-4VP)

The synthesis conditions of cellulose-*g*-poly(4VP-co-BMA) were investigated. The studied reaction conditions included the weight ratio of cellulose and the monomers, reaction temperature, reaction time, amount of the initiator, amount of the crosslinker, and molar ratio of the two monomers, 4VP and BMA. The effects of these reaction conditions on GP and GE are presented in Figure 1.

Figure 1(a) shows the effect of the weight ratio of the cellulose and monomers on GP and GE. In the reaction, the weight ratio of APS/MBA/(4VP+MBA) was 5:0.5:100, and the molar ratio of the two monomers (4VP/BMA) was 2:1. The weight ratio of the cellulose to the monomers was changed by an increase in the weight ratio of cellulose in the reactants. As shown in Figure 1, GP decreased with increasing cellulose/monomer weight ratio, whereas GE increased. The results could be understood as follows. At low cellulose/monomer weight ratios, the relative amount of cellulose was high, and GP decreased because of the increase in the relative amount of cellulose in the reactants. However, GE increased because the increasing amount of cellulose statistically provided more functional groups onto which the monomers could graft. The GE curve leveled off at a weight ratio of 20%; this indicated the saturation of the active free radicals of the monomers. GE was a parameter that was used to evaluate the percentage of monomers in the reactants that has been grafted on the celluloses. In this case, the optimum cellulose/monomer weight ratio was about 20%.

Figure 1(b,c) shows the effect of the temperature and the reaction time on GP and GE. For the results shown in Figure 1(b), the weight ratio of the reactants, cellulose/APS/MBA/(4VP + BMA), was 7:5:0.5:100, and the molar ratio of 4VP/BMA was 2:1. The reaction time in Figure 1(b) was 4 h. The same weight ratio of the reactants was used for the experiments shown in Figure 1(c), and there, the reaction was performed at 70°C. In Figure 1(b), the reaction temperature was investigated in the range of 20–80°C. The result shows that

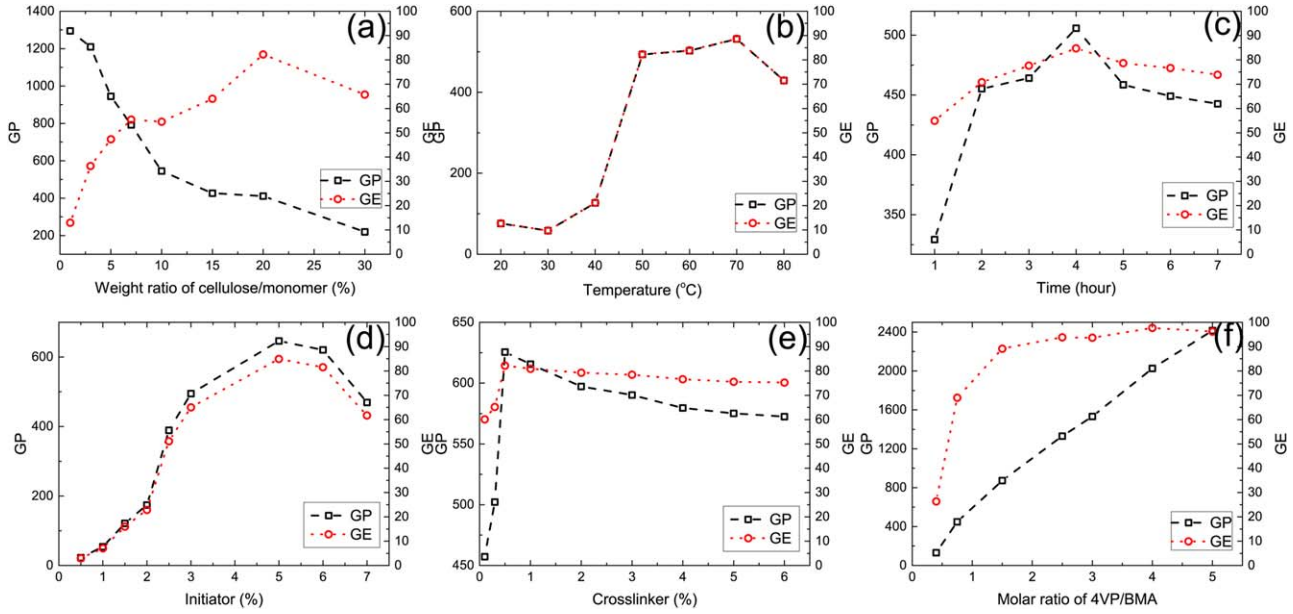

Figure 1. Effect of the reaction conditions on GP and GE. The studied reaction conditions included the (a) cellulose/monomer weight ratio, (b) reaction temperature, (c) reaction time, (d) amount of initiator (APS), (e) amount of crosslinker (MBA), and (f) molar ratio of 4VP/BMA. [Color figure can be viewed in the online issue, which is available at wileyonlinelibrary.com.]

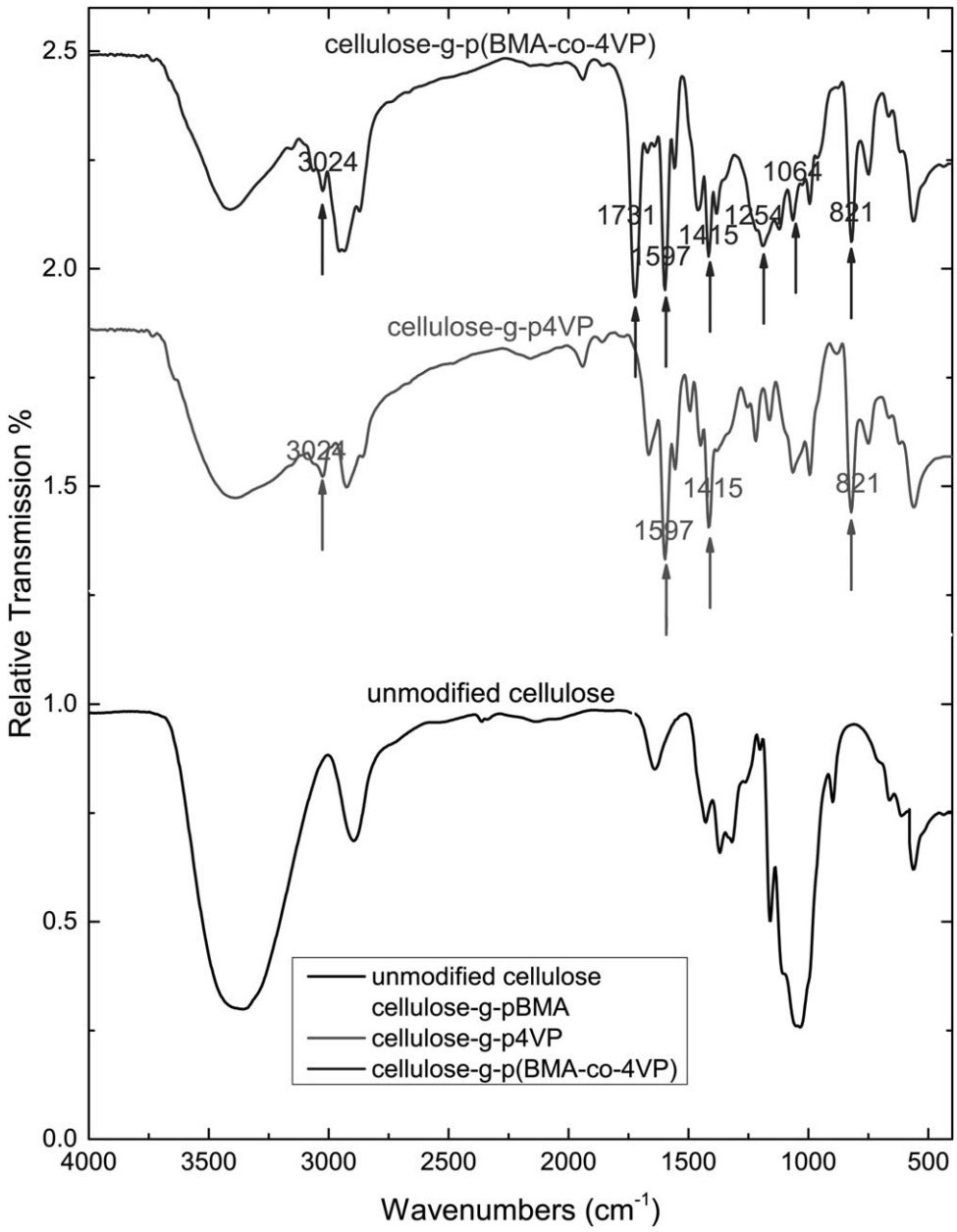

Figure 2. FTIR spectra of the cellulose, cellulose-*g*-pBMA, cellulose-*g*-p4VP, and cellulose-*g*-p(BMA-*co*-4VP). [Color figure can be viewed in the online issue, which is available at wileyonlinelibrary.com.]

when the yield of the reaction increased with the reaction temperature, this was due to both the decrease in the viscosity of the solvent and the increase in the radical propagation rate constant.[15] There was an abrupt increase in GP and GE in the curves between 40 and 50°C, and this indicated the lowest energy required for triggering the radical reaction was between 40 and 50°C. Above 50°C, the effect of the temperature was no longer significant with regard to the increases in GP and GE. Because of the instability of the cellulose at high temperature, the recommended temperature for the grafting was between 50 and 70°C. In Figure 1(c), the effect of the reaction time is evaluated. A prolonged reaction time generally leads to nearly complete monomer conversion. In our case, the influence of the reaction time on the monomer conversion was not considerable when the reaction temperature was 70°C. By 1 h, GE was nearly 60%. With further prolongation of the reaction time, the highest conversion of the monomers was obtained in 4 h. The fast conversion of the monomers was presumably due to the high reaction temperature. Thus, the reaction temperature and the reaction time may have had a synergistic effect on the reaction.

The dependence of GP and GE on the amount of initiator and crosslinker is presented in Figure 1(d,e). For the results shown in Figure 1(d), the reaction conditions were as follows. The weight ratio of the reactants, cellulose/MBA/(4VP + BMA), was 7:0.5:100, and the molar ratio of 4VP/BMA was 2:1. The

reaction was performed at 70°C, and the reaction time was 4 h. For the most common case of radical chain polymerization, the polymerization rate was dependent on the square root of the initiator concentration. As to the final product, it was also dependent on the deactivation of the free radicals during the reaction. Here, we studied the effect of the initiator on the final yield, and the amount of initiator in the reactants was in the regime of 0.5–7 wt %. The concentration of the initiator had a significant effect on the degree of polymerization. At the low concentration of the initiator, the initiation only happened at few sites, and GP and GE were rather low in this case. GP and GE increased with the concentration of the initiator, as shown in Figure 1(d). However, in comparison to the situation when more sites were initiated, the grafted polymer chain presumably grew longer with few initiated sites on the cellulose because the same amount of monomers was present. Figure 1(e) shows the dependence of GP and GE as a function of the crosslinker concentration. The reason to add the crosslinker was to crosslink the backbone of the cellulose, and then, the separation of the final products became feasible by filtration. The reaction conditions for the results shown in Figure 1(e) are as follows. The weight ratio of cellulose/APS/(4VP+BMA) was 7:5:100, and the molar ratio of 4VP/BMA was 2:1. The reaction time was 4 h, and the reaction temperature was 70°C. The results suggest that a small amount of the crosslinker in the reactants benefited the reaction; whereas a further increase in the crosslinker concentration led to decreases in GP and GE. The crosslinking of the cellulose backbone may have reduced the space in the microporous structure, and the diffusion of the monomers in the matrix of the reaction may have been retarded and rendered the decreases in GP and GE.

Figure 1(f) shows the results of GE and GP through changes in the molar ratio of the monomers in the reactants. The weight ratio of the reactants, cellulose/APS/MBA/(4VP + BMA), was 7:5:0.5:100. The reaction time was 4 h, and the reaction temperature was 70°C. The molar ratio of 4VP/BMA was within the range of 0.5 to 5. The results show monotonic increases in GP and GE with increases in the relative amount of 4VP in the reactants. These results clearly exhibit that the addition of 4VP increased the conversion of the monomers. When the molar ratio of 4VP/BMA was above 2, GE approached the total conversion of the monomers. In the study, we were not able to evaluate the molar ratio of the monomers in the final product. However, when GE was nearly 100%, the molar ratio of the monomers in the grafting copolymer should have been the same as it was in the reactants. On the basis of the previous results, the optimum conditions for synthesizing cellulose-*g*-poly(BMA-*co*-4VP) were as follows: the weight ratio of the reactants, cellulose/APS/MBA/(4VP+BMA), was 7:5:0.5:100; the molar ratio of 4VP/BMA was 3:1; the reaction temperature was 70°C; and the reaction time was 4 h. The grafted cellulose used in the characterization and the adsorption studies was synthesized with these optimum conditions.

Characterization of the Grafted Celluloses

FTIR Characterization. The FTIR spectra of the cellulose, cellulose-*g*-poly(butyl methacrylate) (pBMA), cellulose-*g*-poly(4-vinyl pyridine) (p4VP), and cellulose-*g*-poly(butyl methacrylate-*co*-4-vinyl pyridine) [p(BMA-*co*-4VP)] are presented in Figure 2. Characteristic absorption peaks for poly(BMA) occurred at 1731 cm^{-1} (C═O stretching vibrations) and 1254 and 1064 cm^{-1}

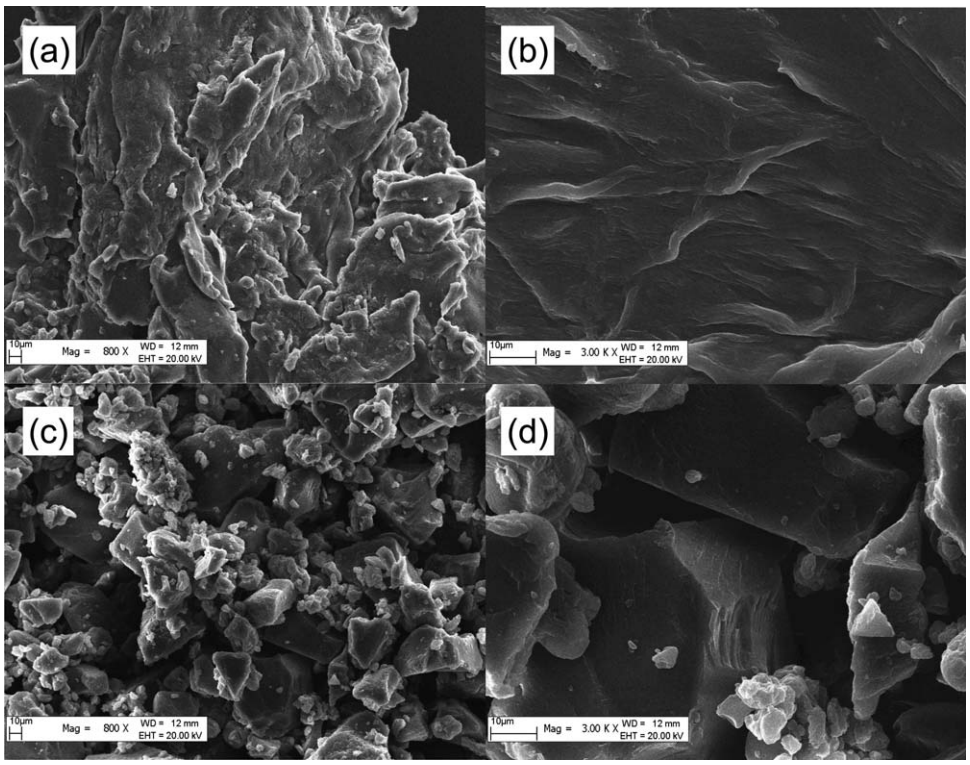

Figure 3. Morphology of the celluloses with magnifications of (a) 800 and (b) 3000× and cellulose-*g*-p(BMA-*co*-4VP) with magnifications of (c) 800 and (d) 3000×.

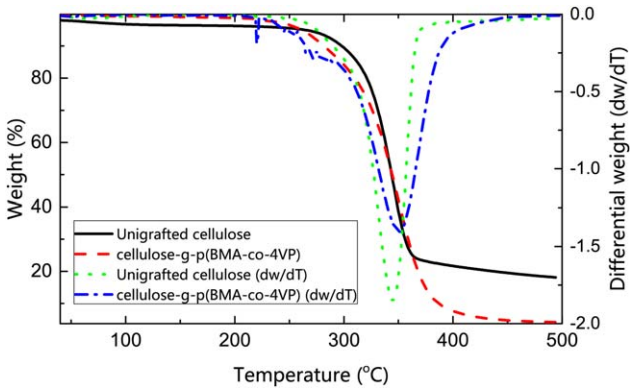

Figure 4. TGA results for cellulose and cellulose-*g*-p(BMA-*co*-4VP). The differential weight loss is presented as a function of the temperature. [Color figure can be viewed in the online issue, which is available at wileyonlinelibrary.com.]

(C—O stretching vibrations); these were visible in cellulose-*g*-pBMA and provided evidence that the grafting of BMA to the cellulose had occurred. The FTIR spectrum of cellulose-*g*-p4VP in Figure 2 shows ligand peaks at 3024 cm^{-1} (C—H stretching vibrations in the pyridine ring), 1597 and 1415 cm^{-1} (in-plane C—H and C—H wagging vibrations in the pyridine ring), and 821 cm^{-1} (symmetric ring breathing). For cellulose-*g*-p(BMA-*co*-4VP), the aforementioned characteristic peaks were all observed, and this was proof of successful grafting.

SEM Characterization. The morphology of the cellulose samples was examined before and after the grafting with SEM. The micrographs of the investigated samples are presented with two different magnifications in Figure 3. The SEM images showed pronounced changes after the grafting. The cellulose samples were dissembled to small granules with the size of tens of micrometers after the grafting, and the grafted celluloses also became rougher on the surface.

TGA Characterization. The TGA results of cellulose and cellulose-*g*-p(BMA-*co*-4VP) and the differential weight loss is presented as a function of temperature in Figure 4; this reflects the difference in the decomposition rates (*dw*/*dT*) for both samples.

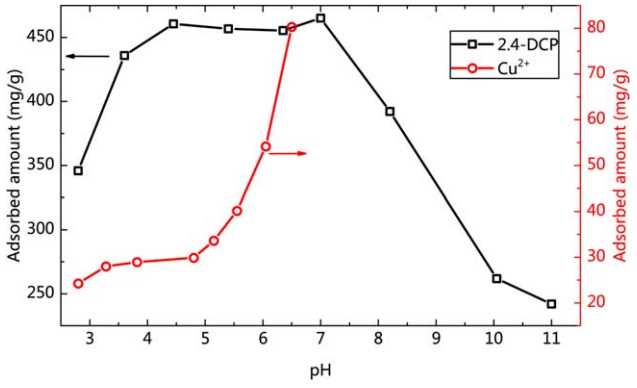

Figure 5. Influence of the solution pH on the adsorbed amount of 2,4-DCP, and Cu(II) is presented as a function of the pH. [Color figure can be viewed in the online issue, which is available at wileyonlinelibrary.com.]

At a temperature around 100°C, the weight loss was attributed to the removal of the water of hydration in the samples. The onset of decomposition of the cellulose was at 255°C, whereas for cellulose-*g*-p(BMA-*co*-4VP), it was at 232°C. The decomposition from 255 to 350°C for the cellulose sample was attributed to the thermal cleavage of the glycosyl groups and the scission of C—O bonds via the free-radical reaction; the decomposition from 232 to 410°C was that of the grafted cellulose.[16] The onset of weight loss for the grafted cellulose was often less than the unmodified one because of the exposure of the grafted copolymers to the cellulose surface. In this case, the microstructure of the cellulose also changed, as shown in Figure 3; this may also have been a reason for the thermal instability. As shown in Figure 4, there was a 20% residual for the cellulose sample after total decomposition; however, the residual was less than 5% for cellulose-*g*-p(BMA-*co*-4VP). With regard to *dw*/*dT*, as shown in Figure 4, the cellulose sample exhibited a more rapid decomposition compared to cellulose-*g*-p(BMA-*co*-4VP). Also, the rapid decomposition of cellulose was at 345°C; it occurred at 351°C for cellulose-*g*-p(BMA-*co*-4VP). The scenario in which the grafted cellulose exhibits a slow decay in the TGA curves is often observed in grafted cellulose.[11]

Results of the Adsorption Experiments

Influence of the pH. The adsorptions of Cu(II) and 2,4-DCP were highly dependent on the pH of the sorbate solutions.

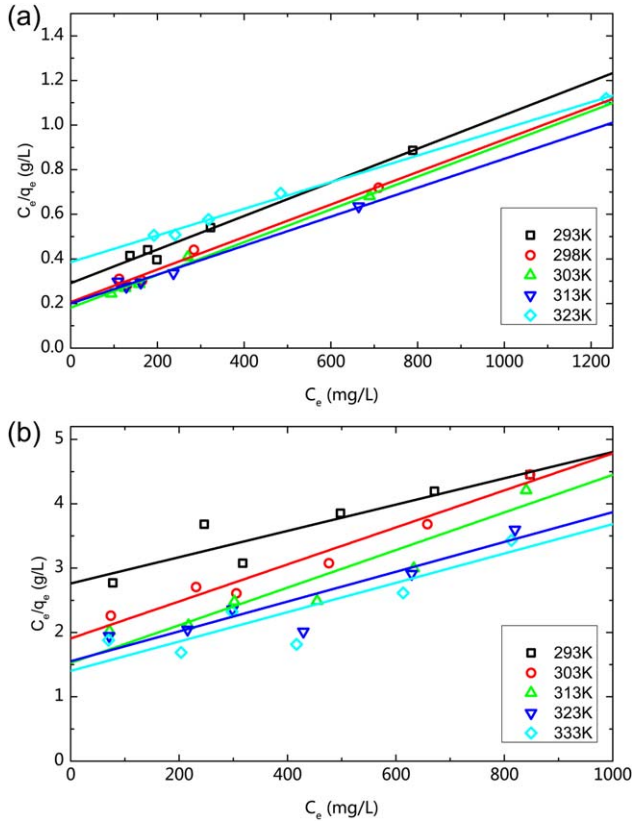

Figure 6. Langmuir adsorption isotherms for (a) 2,4-DCP and (b) Cu(II) adsorption on cellulose-*g*-p(BMA-*co*-4VP). The temperatures of the experiments were in the regime 293–333 K. [Color figure can be viewed in the online issue, which is available at wileyonlinelibrary.com.]

Changing pH may affect the state of ionization and also the surface charge of the grafted cellulose. The adsorbed amounts of Cu(II) and 2,4-DCP were tested with the variation of the initial pH of the sorbate solutions, and the results are shown in Figure 5. The test for the removal of Cu(II) was studied by the variation of the pH between 2.8 and 6.5; for removal of 2,4-DCP, the variation of pH was between 3.0 and 11.0. In the case of Cu(II), the adsorbed amount exhibited a monotonic increase with the initial pH of the solution. This was caused by the weakening of the competitive binding between H^+ and Cu(II). When the pH of the solution increased above 5.5, the increase in the adsorbed amount of Cu(II) was due to the precipitation of $Cu(OH)_2$; this should not have been perceived as the adsorption of Cu(II) on the grafted cellulose. For 2,4-DCP, the adsorbed amount remained nearly constant at pH 4.0–7.0. As the pH increased, 2,4-DCP exhibited an increasingly negative characteristic, which led to an increase in the solubility, and also, the adsorption of 2,4-DCP was presumably due to the interaction with the hydrophobic domains on the grafter. Therefore, the adsorbed amount of 2,4-DCP started decreasing when the pH value was above 7.0.

Adsorption Isotherms. The adsorption experiments were performed with different initial concentrations of the adsorbates at different temperatures to obtain the adsorption isotherms. As mentioned previously, an adsorbate binds to an adsorbent through many mechanisms. In our case, the Cu(II) ions were adsorbed to the grafted cellulose presumably by chelation and to 2,4-DCP by hydrophobic interactions. Both of the mechanisms required the binding sites to be free and the active site to be occupied only by one adsorbate molecule; this satisfied the precondition of the Langmuir model of adsorption. Therefore, we applied the Langmuir adsorption model by performing a linear regression of the experimental data to the Langmuir isotherm:

$$\frac{c_e}{q_e} = \frac{c_e}{\Gamma_{max}} + \frac{1}{k\Gamma_{max}} \tag{4}$$

where k is the adsorption constant and Γ_{max} is the maximum adsorption at equilibrium. The two later parameters were obtained by the linear regression of the following relation:

$$\frac{c_e}{q_e} \sim c_e \tag{5}$$

These values are presented in Figures 6(a,b) for 2,4-DCP and Cu(II), respectively. The results of the maximum adsorption are presented in Figure 7 as a function of the temperature. The maximum adsorption for 2,4-DCP exhibited a linear relation with temperature; this confirmed that the hydrophobic interaction was the primary mechanism of the adsorption for 2,4-DCP. For Cu(II), the maximum adsorption was independent of the temperature because the predominant cause of chelation was the entropy contribution.

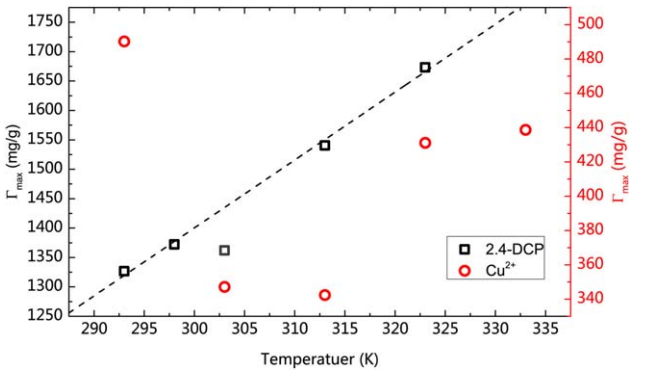

Figure 7. Maximum adsorption amounts of 2,4-DCP and Cu(II) obtained by the regressions of the Langmuir isotherm are presented as a function of the temperature. [Color figure can be viewed in the online issue, which is available at wileyonlinelibrary.com.]

The values of k were determined by a linear regression of the Langmuir isotherm. We used the temperature dependence of k to determine the standard free energy (ΔG) and isosteric enthalpy of adsorption (ΔG; the standard enthalpy of adsorption at a fixed surface coverage) and, thereby, the standard entropy (ΔS). The relationship of these thermodynamic parameters is given as follows:

$$\Delta G = -RT\ln k = \Delta H - T\Delta S \tag{6}$$

$$\left[\frac{\partial \ln k}{\partial(1/T)}\right] = \frac{\Delta H}{R} \tag{7}$$

where R is the gas constant and T is the temperature.[17] The calculated values of the thermodynamic parameters are outlined in Table I. The obtained values of the thermodynamic parameters further confirmed the mechanism of the adsorption of 2,4-DPC and Cu(II). As shown in Table I, the standard enthalpy and entropy for 2,4-DPC were positive; this is typical for hydrophobic interactions. The entropy increase in the hydrophobic interaction was due to the fact that some of the hydrogen bonds that formed the clathrate cage by water molecules were broken. For the adsorption of Cu(II), the standard enthalpy and entropy were negative; this indicated that the entropy contribution in the adsorption of Cu(II) was unfavorable, and the reaction absorbed heat from the environment. This is representative in chelation.

Kinetics of Adsorption. The kinetics of adsorption were also investigated. In the literature, the kinetics of the adsorption have been described by kinetic models, such as the pseudo-first-

Table I. Thermodynamic Parameters for the Adsorption of 2,4-DCP and Cu(II) on Cellulose-*g*-p(BMA-*co*-4VP)

	ΔG (kJ/mol)							
	293 K	298 K	303 K	313 K	323 K	333 K	ΔH (kJ/mol)	ΔS (J K^{-1} mol^{-1})
2,4-DCP	−14.3	−14.9	−15.3	−15.8	−15.7		1.76	55.6
Cu(II)	−9.88		−10.2	−10.8	−11.4	−11.9	−12.5	−53.8

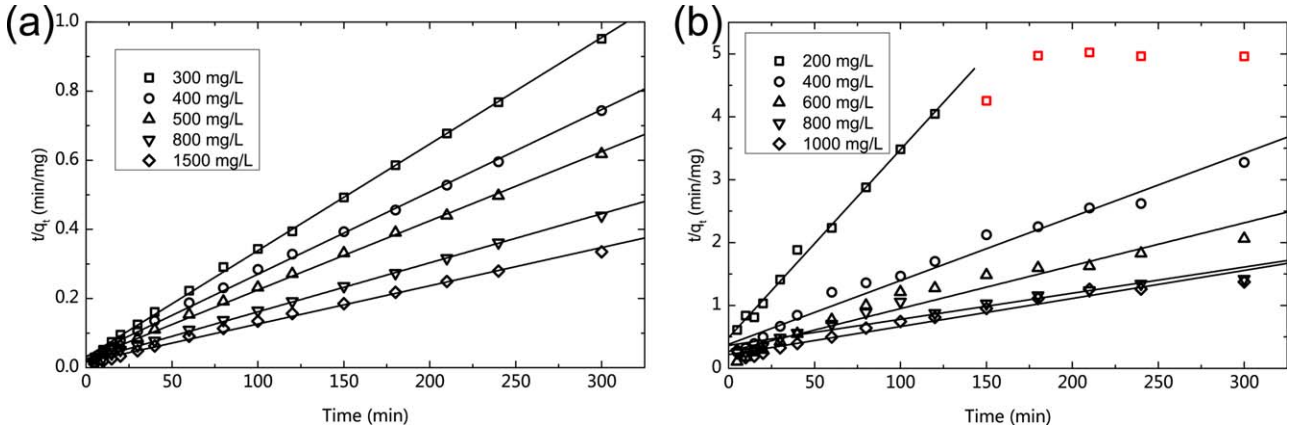

Figure 8. Pseudo-second-order adsorption kinetics of (a) 2,4-DCP and (b) Cu(II) on cellulose-*g*-p(BMA-*co*-4VP) at different initial concentrations. The experiments were conducted at 297 K.

order model, pseudo-second-order model, and diffusion model. We mentioned previously that the adsorption of 2,4-DCP was only on the surface of the celluloses, and for Cu(II), the adsorption might have been caused by the diffusion in the cellulose in addition, which would be reflected in the kinetic study. The results of the kinetic studies are presented in Figure 8. The studied time region was within the contact time for equilibrium adsorption, and the initial concentration of the adsorbates was below the maximum amount that the adsorbent could take up. The pseudo-second-order model was used to analyze the adsorption data, as represented in linear form with the following equation:

$$\frac{t}{q_t} = \frac{1}{q_e^2 k_2} + \frac{t}{q_e} \tag{8}$$

where q_t represents the adsorbed amount at time t and k_2 is a rate constant for the adsorption process. For the case of the adsorption of 2,4-DCP, t/q_t showed a linear increase with time t in the studied time region. The plots presented high correlation coefficients and good compliance with the pseudo-second-order model, as shown in Figure 8(a). The obtained adsorbed amount at equilibrium and the adsorption rate are presented in Table II. We found that q_e increased and k_2 decreased with the initial concentrations of the adsorbates for 2,4-DCP. From the results presented in Table II, the adsorption of 2,4-DCP on cellulose-*g*-p(BMA-*co*-4VP) was rather complete, especially at low initial concentrations.

Table II. Parameters of the Linear Regression Shown in Figure 8

2,4-DCP			Cu(II)		
C (mg/L)	q_e (mg/g)	k_2 (g mg^{-1} L^{-1})	C (mg/L)	q_e (mg/g)	k_2 (g mg^{-1} L^{-1})
300	324	3.12×10^{-4}	200	33.4	1.83×10^{-3}
400	420	1.77×10^{-4}	400	98.7	2.68×10^{-4}
500	500	1.62×10^{-4}	600	146	1.73×10^{-4}
800	704	1.03×10^{-4}	800	241	4.72×10^{-5}
1500	900	7.86×10^{-5}	1000	224	9.05×10^{-5}

C, initial concentration of the adsorbate.

As to the Cu(II) adsorption, the results of the adsorption kinetics are presented in Figure 8(b). We observed that the Cu(II) adsorption clearly involved two process, especially at a low initial concentration. The initial adsorption obeyed the pseudo-second-order model, where t/q_t increased linearly with time. After a critical time, the value of t/q_t became independent of the time, as shown in Figure 8(b) (the red symbols). This indicated that a different mechanism drove the adsorption; this was presumably the diffusion of Cu(II) in the cellulose. Detailed information was only observed for the adsorption with the low initial concentration (200 mg/L) of Cu(II). For the samples with higher initial concentrations, the two-step adsorption could still be distinguished; however, the adsorption due to diffusion became negligible. Thus, only the initial adsorption process was analyzed by the pseudo-second-order model for the sample with 200 mg/L Cu(II), and the linear regression was performed with the data in the full time range for the rest of the samples. The results are presented in Table II. Compared to the adsorption of 2,4-DPC, the adsorption capacity of Cu(II) was considerably lower. The adsorption capacity was roughly calculated as follows: 1 g of the adsorbent could remove one-quarter of the adsorbate in a 1-L solution. However, the uptake of Cu(II) by cellulose-*g*-p(BMA-*co*-4VP) was substantially higher comparing with commercial adsorbent/ion-exchange materials (the highest Cu(II) uptake was 130 mg/g, as presented in ref. [3).

CONCLUSIONS

In this study, three grafted celluloses, including cellulose-*g*-pBMA, cellulose-*g*-p4VP, and cellulose-*g*-p(BMA-*co*-4VP), were synthesized and applied to remove Cu(II) and 2,4-DCP from water, respectively. The optimum conditions for synthesizing cellulose-*g*-poly(BMA-*co*-4VP) were acquired by an investigation of the effects of the weight ratio of the reactants, the reaction temperature, and the reaction time on the yields. The adsorption isotherms were interpreted with the Langmuir adsorption model. For 2,4-DPC, the standard enthalpy and entropy were

positive, whereas those for Cu(II) were negative. The kinetics data demonstrated that the removal of 2,4-DCP followed a pseudo-second-order reaction rate, whereas the adsorption of Cu(II) was a two-step process. These findings suggest that cellulose-*g*-p(BMA-*co*-4VP) exhibits great potential as an adsorbent in the removal of both phenols and heavy-metal ions and also confirmed the strategy of the grafting of different monomers onto celluloses to achieve multiple objectives.

ACKNOWLEDGMENTS

W.W. acknowledges the TianShan and QianRen Project for financial support. R.L.W. acknowledges the National Natural Science Foundation of China (contract grant number 51063007) for financial support.

REFERENCES

1. Verlicchi, P.; Al Aukidy, M.; Zambello, E. *Sci. Total Environ.* **2012**, *429*, 123.
2. Li, Y.; Zhu, G.; Ng, W. J.; Tan, S. K. *Sci. Total Environ.* **2014**, *468–469*, 908.
3. O'Connell, D. W.; Birkinshaw, C.; O'Dwyer, T. F. *Bioresour. Technol.* **2008**, *99*, 6709.
4. Clark, M. M.; Ahn, W. Y.; Li, X.; Sternisha, N.; Riley, R. L. *Langmuir* **2005**, *21*, 7207.
5. Habibi, Y. *Chem. Soc. Rev.* **2014**, *43*, 1519.
6. Wang, W.; Sande, S. A. *Langmuir* **2013**, *29*, 6697.
7. Fu, F. L.; Wang, Q. *J. Environ. Manage.* **2011**, *92*, 407.
8. Wu, R. L.; Wang, X. L.; Li; F.; Li, H. Z.; Wang, Y. Z. *Bioresour. Technol.* **2009**, *100*, 2569.
9. Wang, W.; Arne Sande, S. *Eur. Polym. J* **2014**, *58*, 52.
10. Ngah, W. S. W.; Hanafiah, M. A. K. M. *Bioresour. Technol.* **2008**, *99*, 3935.
11. O'Connell, D. W.; Birkinshaw, C.; O'Dwyer, T. F. *J. Appl. Polym. Sci.* **2006**, *99*, 2888.
12. Sud, D.; Mahajan, G.; Kaur, M. P. *Bioresour. Technol.* **2008**, *99*, 6017.
13. Lin, S. H.; Juang, R. S. *J. Environ. Manage.* **2009**, *90*, 1336.
14. Zhang, H.; Wu, J.; Zhang, J.; He, J. S. *Macromolecules* **2005**, *38*, 8272.
15. Wang, J.-S.; Matyjaszewski, K. *J. Am. Chem. Soc.* **1995**, *117*, 5614.
16. Huang, M.-R.; Li, X.-G. *J. Appl. Polym. Sci.* **1998**, *68*, 293.
17. Atkins, P.; de Paula, J. Atkins' Physical Chemistry; Oxford University Press: Oxford, England, **2014**.